

Reconstruction of the vector fields of continuous dynamical systems from numerical scalar time series

G. Gouesbet

*Laboratoire d'Énergétique des Systèmes et Procédés, Institut National des Sciences Appliquées de Rouen,
Boîte Postale 08, 76131 Mont Saint Aignan CEDEX, France*

(Received 4 September 1990; revised manuscript received 4 December 1990)

We emphasize that the ordinary differential equations of a continuous dynamical system, or at least of equivalent systems, can be reconstructed from numerical scalar time series. Methods are exemplified in the case of a strange, chaotic attractor generated by a mathematical model, namely, a Rössler band. Resultant validations rely (i) qualitatively on comparisons between original and reconstructed phase portraits, and (ii) quantitatively on comparisons between generalized dimensions D_q of original and reconstructed attractors. Some of the many lines of research offered by the presented results are discussed to stress potentialities of this kind of reconstruction.

I. INTRODUCTION

There is now a great interest in the study of the theory of nonlinear dissipative dynamical systems, with applications to several miscellaneous fields, including, for instance, mechanics of structures, hydrodynamics, general physics, chemistry, biology, ecology, epidemiology, and economics. Indeed, the number of actual and potential applications of nonlinear dynamics is tremendously big because most systems existing in nature may be described by mathematical models such as nonlinear maps and flows. To gain a background knowledge on such topics, the reader may consult textbooks such as those by Guckenheimer and Holmes,¹ Thompson and Stewart,² Devaney,³ or Bergé, Pomeau, and Vidal,⁴ and also increasingly prolific literature.

Particular attention is paid to systems producing strange and chaotic attractors, the words strange and chaotic here referring to metric properties, i.e., fractal dimensions, and to dynamical properties, i.e., sensitivity to initial conditions, respectively. In such cases, dissipative phenomena previously attacked in terms of high-dimensional phase spaces and/or of noise sources may be actually understood in low-dimensional phase spaces as the consequence of deterministic chaos. When studying experimental systems, a single scalar variable is usually recorded versus time. Therefore a great deal of effort has been devoted to the quantitative characterization of underlying attractors when our knowledge of the system is limited to a recorded numerical scalar time series.

There exists a host of invariants to quantify attractors, such as natural measure, pointwise and partial dimensions, Hausdorff dimension, or Lyapunov exponents (see Refs. 5–7, for instance). Now the most popular quantities might be generalized dimensions D_q , generalized entropies K_q , and their associated singularity spectra. Also, there are now several well-known algorithms available to derive these quantities from numerical scalar time series relying, for instance, on fixed-radius or fixed-mass approaches, or on the determination of unstable periodic orbits that are dense in the attractor (see Refs. 8–19, for

instance, and references therein).

The above evaluations are purely numerical and require the reconstruction of attractors in phase spaces of dimensions n usually much bigger than the minimal dimension n_0 . There is one theoretical and one practical reason, implying that n must usually be bigger than n_0 . Theoretically, we have a theorem of Mañé²⁰ and Takens^{21,22} stating that the points of the attractor may be parametrized by n real coordinates if $n \geq n_T$ in which n_T is given by the Takens criterion $n_T = 2D + 1$. Here, D can be taken as being the Hausdorff dimension D_H or the capacity D_K of the set. One recalls that, for every compact set S , $D_H(S) \leq D_K(S)$.²³ In practice, D is often taken as being the correlation dimension D_2 of the attractor, which may be rather easily evaluated. A rough but not too misleading evaluation is to take D as being the dimension n_0 of a minimal embedding phase space. Takens's criterion, however, gives a sufficient condition because many manifolds and attractors contained in them having a typical dimension D can be embedded in less than n_T -dimensional phase spaces. Although this paper is devoted to flows, we stress that the above discussion extends to the case of maps.

Practically however, for a phase space of dimension n satisfying Takens's criterion, the quality of the reconstruction is not warranted. Sophisticated procedures like singular value decomposition or redundancy analysis may be used to approach the best reconstruction,^{24–27} but there also exists a simple pragmatic method relying on the observation that the value of the so-called window length is determinant in the quality of the projection process.^{13,24} We then find that the dimension n_p of the phase space in which the attractor is reconstructed must be in practice much bigger than n_T to avoid biased evaluations such as severe underestimations. For instance, we may consider an attractor generated by a simple model of thermal lens oscillations.²⁸ The original phase space is of dimension 3 and generalized dimensions D_q of the attractor are equal to about 2. Therefore, n_T is about 5. The optimal phase-space dimension n_p relying on the

window-length approach is, however, 25. The problem is similar for generalized entropies K_q because evaluation of these quantities from time series requires the computation of order q correlations (see Sec. III C) for phase spaces of increasing dimensions. For instance, in Ref. 28, again, these dimensions range up to 45.

When dealing with experimental systems, data requirements for running the algorithms may then become prohibitive. These data requirements become more stringent when high-dimensional phase spaces are required because data points are spread in hypervolumes of bigger dimensions. As a result of these difficulties, time series may even be possibly erroneously diagnosed as being chaotic.

When the algorithms are successful, there is no doubt that they provide us with valuable information. We may have concluded that the system is deterministic. We may also have obtained interesting data to discuss the forecasting issue from Lyapunov exponents and/or generalized entropies. For instance, the largest Lyapunov exponent tells us how far into the future reliable predictions are feasible. We may finally have evaluated the effective number of degrees of freedom required to describe the dynamics telling us what the minimal dimension n_0 of the embedding phase space may be, i.e., how many ordinary differential equations we need to produce a phenomenological model of the system (see a later discussion in Sec. II A). However, even then, we remark, in agreement with Casdagli,²⁹ that the calculated invariants are of limited practical interest. This is an especially disappointing state of affairs when we consider the large amount of skill involved in the underlying mathematics and associated numerical expertise. In particular, even if we determined n_0 , a necessary bit of information for the construction of a model, we would not know how to construct the model itself from the available time series.

For modeling purposes, we usually have to rely on physics and on the understanding of instability mechanisms, independently of the knowledge of any time series. An example concerning thermal lens oscillations and associated hot-wire phenomena^{30–32} is described in Refs. 28 and 33. Afterward, we must compare the model and experimental data and possibly iterate between theory and experiments up to the obtainment of a satisfactory enough agreement. This is a lengthy, inconvenient and tedious procedure. Furthermore, if we have to study a new system, we must build a new model starting from new principles relevant to the new system under study, i.e., each system is really a special case.

In this paper, we emphasize that it is possible to overcome all the aforementioned shortcomings because the knowledge of numerical scalar time series enables us to reconstruct the original vector field equations, or at least equations equivalent to them. Therefore there are more or less systematic algorithms for building phenomenological models from scalar time series. Since our methods are exemplified on a rather simple case, we clearly expect that variants will be produced in the future and that they will be actually needed to investigate more and more complicated vector fields. But we expect that most of the essential ideas will be preserved. We shall, however, dis-

tinguish between what is particular to the studied example and therefore should be generalized to attack more difficult cases, possibly making suggestions for these generalizations, and what is expected to be robust.

When the model is constructed, we obtain a continuous dynamical system evolving in a phase space of minimal dimension n_0 . Therefore, metric and dynamical properties of attractors may be computed in R^{n_0} , leading to less stringent requirements than having to work with a phase space of dimension $n_p > n_T > n_0$. There may be also some other opportunities, which are listed below, but those we shall not explicitly consider in this paper. Flow predictions by using reconstructed systems become feasible, and we expect that the corresponding techniques could also be applied to map predictions (see Refs. 29 and 34) by lifting them to flows. Although the system is originally known from only a time series, bifurcations of the system might be predicted by studying the properties of the reconstructed vector fields. Some of these statements may be optimistic but only further work will determine how far we may go in the proposed directions.

We note that our methods require the computation of time derivatives. Time derivatives have been widely used to evaluate attractor invariants in reconstructed phase spaces, although the so-called time-delay technique is now more popular, but without considering the issue of vector field reconstructions. Nevertheless, the possibility of vector field reconstruction has been briefly discussed by Packard *et al.*³⁵ on the example of the Rössler system and used to evaluate a characteristic exponent. However, no systematic development of the idea is given. Later on, Cremers and Hübler³⁶ provide a more systematic discussion of the same idea and consider the case of a Lorenz attractor and of a van der Pol oscillator. The structure of the original vector fields is, however, assumed to be known, and a test of the quality of results only relies on the determination of a limit cycle radius. The issue of strange attractors is not examined. These two references must nevertheless be considered as precursors of our own contribution.

The paper is organized as follows. Section II defines the chosen system to study, introduces algorithms, and applies them to the production of reconstructed systems. Section III provides us with qualitative and quantitative validations. Section IV is a conclusion.

II. ALGORITHMS AND RECONSTRUCTED SYSTEMS

A. The system under study and the standard transformations

We consider the example of a Rössler band generated by the following equations:

$$\begin{aligned}\dot{x} &= -y - z \\ \dot{y} &= x + ay, \\ \dot{z} &= b + z(x - c),\end{aligned}\tag{1}$$

with control parameter values $a=0.398$, $b=2$, $c=4$, for which the asymptotic motion of the system settles down on a strange, chaotic attractor when initial conditions are

chosen in the basin of attraction.² Rössler equations are particularly simple, displaying only one nonlinear vector field component, and therefore provide us with an easier opportunity to illustrate basic methods. Although our final motivation is the study of noisy experimental systems, testing a simple case is a prerequisite before attacking more difficult situations. We also choose the case of a chaotic attractor, which represents the most interesting issue to investigate. For limit cycles, see Cremers and Hübner.³⁶

From integration of the system by a fourth-order Runge-Kutta algorithm, we obtain a numerical scalar time series $\{x_i\}$ that represents the asymptotic chaotic motion when transients have been allowed to die. This time series is assumed to be all the knowledge we possess concerning the motion of the system. From it, we intend to reconstruct the original system (1) or at least systems equivalent to it.

An example of an equivalent system (in some sense) is provided by what we call the direct standard transformation (DST), which is a change of coordinates taking original coordinates (x, y, z) to new ones (x, Y, Z) according to

$$\begin{aligned}\dot{x} &= Y, \\ \dot{Y} &= Z, \\ \dot{Z} &= F(x, Y, Z).\end{aligned}\quad (2)$$

In principle, we are not supposed to know the number of equations required for the standard reconstructed system (SRS) defined by Eq. (2). Therefore, when the original system is unknown, we must start with a preliminary evaluation of the number of degrees of freedom from time series $\{x_i\}$. There are many opportunities to fulfill this task. When using singular-value decomposition,²⁴⁻²⁶ series $\{x_i\}$ are used to construct an orbit matrix made of N rows, each row being an n -dimensional vector obtained by embedding the series in an n -dimensional reconstructed phase space. In principle, i.e., not withstanding additional difficulties as due to the presence of noise, the number of coordinates required to define the state system is equal to the rank of the orbit matrix. Also, the minimal dimension of the required phase space is closely related to a fractal dimension D of the attractor. For instance, according to Froehling *et al.*,³⁷ to determine the dimension of a low-dimensional attractor, only a few independent quantities are needed: as few as the fractal dimension D of the attractor rounded to the next integer. The same idea is discussed by Farmer, Ott, and Yorke,⁵ stating that the dimension of an attractor is a lower bound on the number of essential variables needed to model the dynamics, and by Cenys and Pyragas,³⁸ who explicitly write the relation $n_0 = \text{int}(D) + 1$ and test it on several examples. However, the multifractal attractor possesses a spectrum of generalized dimensions D_q rather than a single dimension D . From this point of view, the most interesting dimension is the minus infinite-order dimension $D_{-\infty}$ (characterizing the domain of the attractor where the measure is most rarefied) because it is an upper bound of all the D_q 's.

In the present case, a proper evaluation with successful

algorithms would provide the correct answer $n_0 = 3$. Then we will elaborate on the economy of this evaluation later in this section (but see Sec. III C). However, we also believe that the algorithms used to construct the SRS (2) contain in principle the possibility of an independent evaluation of n_0 from the time series. This belief relies on the idea that, if the number of equations is too big, evaluations of constants associated with reconstruction will be dominated by numerical noise and will vary much when different series are investigated. We similarly expect nonreproducibility of results with respect to different time series if the number of equations is too small. Therefore our methods might also provide a way to determine the minimal dimension n_0 . Examples of noise-dominated and nonreproducible constant evaluations will be discussed in Sec. II C.

The basic idea is now as follows. From scalar time series $\{x_i\}$, we may determine vectorial time series $\{x_i, Y_i, Z_i, \dot{Z}_i\}$. In this paper, this is done by using a centered finite-difference scheme with a time step δt equal to the time step in the Runge-Kutta algorithm used for integration, i.e., for instance,

$$\dot{x}_i = Y_i = (x_{i+1} - x_{i-1}) / 2\delta t. \quad (3)$$

We are then left with the problem of determining the unknown function F . It is of further interest to know how the original Rössler system (1) is theoretically transformed by the DST. We readily find that the standard coordinates Y and Z are given by

$$Y = -y - z, \quad (4)$$

$$Z = -b - x - ay + z(c - x), \quad (5)$$

and establish that the function F reads

$$\begin{aligned}\dot{Z} &= ab - cx + x^2 - axY + xZ + (ac - 1)Y + (a - c)Z \\ &\quad - \frac{Y}{a + c - x}(x + b - aY + Z).\end{aligned}\quad (6)$$

We note that there is seemingly a singularity in the standard exact system (SES) at $x_c = a + c$ [Eq. (6)]. A closer inspection would, however, reveal that this singularity is only apparent.

For unknown original vector field cases in which all the available information is contained in time series $\{x_i\}$, reconstruction leads to SRS's [Eq. (2)]. From the standard reconstruction using coordinates (x, Y, Z) , we are also free to consider any inverse transformation taking standard coordinates (x, Y, Z) to new ones (x', y', z') . An interesting line of research would be to know whether our finding inverse transformations such as coordinates (x', y', z') had a clear physical meaning.

Among all the inverse transformations, there is a special one, the inverse standard transformation (IST), taking back the standard coordinates (x, Y, Z) to the original ones (x, y, z) . In the present case, where the original system is known, the IST is known and defined below. We use Eqs. (4) and (5) and the trivial relation $x = x$. Furthermore, we demand that the last two equations for \dot{y} and \dot{z} of the original system (1) be exactly satisfied. Therefore, all numerical errors associated with reconstructions are

reported on the first equation for \dot{x} . For a given reconstruction, the IST then produces an inverse standard reconstructed system (ISRS), taking the form

$$\begin{aligned}\dot{x} &= F'(x, y, z), \\ \dot{y} &= x + ay, \\ \dot{z} &= b + z(x - c).\end{aligned}\quad (7)$$

In this paper, the interest in considering vector fields and attractors generated by the IST lies in the fact that it allows for more direct and convincing validations of reconstructions, because, if reconstructions [i.e., determination of F in (2)] were perfect, the IST would enable us to perfectly recover the original Rössler system (1).

In summary, in the present case when the original system is known, and also in all cases when it is unknown, the function F of the standard system (2) may be determined with some accuracy. We may afterward examine the vector fields and the attractors generated by the standard system and also by any inverse transformation we like. In the present paper, after having evaluated function F (a step valid in all cases), we will make the choice of examining vector fields and attractors generated by the IST, in order to test the quality of our methods against the behavior of the known original Rössler attractor. Discussion of attractors generated by standard systems and by subsequent inverse transformations using coordinates $(x', y', z') \neq (x, y, z)$ is postponed to a future work.

B. Research of F by using ratios of polynomial expansions

When the original system is unknown, the determination of the standard function F should rely on the decomposition of F on a complete set of orthogonal functions, with the issue being to determine which set would be the best, i.e., leading to fast convergence and easy numerics. An example of such a decomposition, using Legendre polynomials for reconstruction of a limit cycle, is provided by Cremers and Hübler.³⁶ In any case, we may also attempt to research F by using ratios of polynomial expansions, according to

$$\dot{Z} = \frac{\sum_{j+k+m=0}^{N_0} N_{jkm} x^j Y^k Z^m}{1 + \sum_{j+k+m=1}^{N_0} D_{jkm} x^j Y^k Z^m}.\quad (8)$$

In the denominator, the term $D_{000}x^0Y^0Z^0$ is set equal to 1 to remove an undetermination in the problem. The general procedure then consists in considering successively increasing orders N_0 of approximations till convergence of the process is obtained. The form (8) and also a simpler form without any denominator (N_0 -order polynomial) have acquired some popularity in forecasting problems.^{29,34} However, we have not succeeded in approximating F with N -order polynomials in our case.

Furthermore, although Eq. (8) may be tested in any case (unknown original system), it is particularly suitable for the present case of the Rössler system, because (6) takes the form (8) with $N_0=3$. Therefore, only computa-

tions at this order will be discussed. Theoretical values of constants N_{jkm} and D_{jkm} (not given) are easily derived. Among these 39 constants, only 13 are not equal to 0. To evaluate constants from time series $\{x_i, Y_i, Z_i, \dot{Z}_i\}$, Eq. (8) is rewritten as

$$\begin{aligned}N_{000} + N_{100}x \\ + N_{010}Y + \dots - D_{012}YZ^2\dot{Z} - D_{111}xYZ\dot{Z} = \dot{Z}.\end{aligned}\quad (9)$$

In practice, about ten quadruplets $\{x_i, Y_i, Z_i, \dot{Z}_i\}$ are sampled per pseudoperiod $T_0 \simeq 6.22$ of the Rössler band. When 39 quadruplets are recorded, Eq. (9) produces a set of linear equations that is solved by the Cramer technique, leading to an evaluation of the set of constants. To provide more accurate results, we actually solve N_s sets of equations. The evaluation of one constant associated with one set is called a realization of the constant. The algorithm for evaluations then proceeds in two steps.

In the first step, we solve N_s^1 sets of equations. For each constant, we compute an evaluation K equal to the average over the N_s^1 realizations and the corresponding standard mean deviation σ [relative root mean square (rms) denoted by α]. The relative rms allows for the evaluation of a statistical accuracy δ given by $\alpha/\sqrt{N_e}$ in which an irrelevant numerical prefactor is omitted. Here, N_e is the number of realizations used to compute the evaluation K , which is equal to N_s^1 in the present first step. For constants that are not theoretically equal to 0, we also compute ϵ , the absolute value of the relative difference between the theoretical value of the constant and its numerically reconstructed value, in order to quantify the accuracy of the evaluation. For constants that are theoretically equal to 0, δ is not computed and ϵ has no meaning. Then, the accuracy of the evaluation is obtained by using Δ , the absolute difference between the theoretical value and the reconstructed value, i.e., the modulus of the reconstructed value itself.

Then, several series $\{x_i, Y_i, Z_i, \dot{Z}_i\}$ with different N_s^1 and different Runge-Kutta time steps are processed. In any case, we observe that evaluations of constants that are theoretically equal to 0 are characterized by very big values of the relative rms α . This fact indicates that these evaluations are dominated by numerical noise. Relying on the results concerning the other constants, we then identify the best series among all the processed series. The best series is defined as the one giving the best, i.e., the smallest, average δ per constant not theoretically equal to 0. This is a statistical objective criterion. It is chosen for the sake of objectivity, even if the best series does not correspond to the smallest ϵ and Δ , because we are not supposed to know these two last quantities. We obtain our best series with $\delta t = 10^{-3}$ and $N_s^1 = 5$. For it, ϵ and Δ are 0.001 and 0.000 15, respectively.

When processing different series with the above first step of the algorithm, we observe that increasing the number of processed sets of equations and/or decreasing

the Runge-Kutta time step do not necessarily improve the results. Indeed, some sets of equations lead to very poor evaluations for some constants. Therefore, result improvement requires the use of a discrimination scheme that is implemented in the second step of the algorithm. This discrimination scheme is based on the results of the first step.

We now solve N_s^2 sets of equations. For each constant, each realization is tested to reject poor evaluations associated with badly conditioned sets. Rejection is based on the evaluation K of the first step and on the value of the associated standard mean deviation σ . If a realization ranges between $K - 2\sigma$ and $K + 2\sigma$, it is accepted. Otherwise, it is rejected. The discrimination acting separately on each constant (not on sets, although this other kind of discrimination is also possible), the rate of rejection depends on the constant. We then define an average rate of rejection per constant. Quantities K , α , ϵ , and δ are evaluated similarly, as in the first step, but only account for validated realizations. To evaluate δ , N_e is taken equal to N_s^2 , corrected by the average rate of rejection. Several series are processed, and we retain the results of the best series defined as in the first step by the smallest average δ

per constant not theoretically equal to 0, i.e., not associated with large relative standard mean deviations.

The best processed series was for $\delta t = 10^{-3}$ with 49 998 quadruplets (i.e., $N_s^2 = 1282$), the rate of rejection depending on the constant ranges between 10% and 34%, with an average rate per constant equal to 17%. Reconstructed numerical values of constants are given in Table I. The average ϵ per constant theoretically not equal to 0 is now 0.000 25, representing a gain of accuracy by a factor of 4 with respect to the first step evaluations. The corresponding average δ per constant is about 10^{-4} . For constants theoretically equal to 0, the average Δ per constant decreases down to 3×10^{-5} , representing a gain of accuracy by a factor of 5. These results seem very satisfactory. At least, they show that a two-step algorithm leads to improved results. Afterwards, starting from the second step, we attempted to similarly use a third step iteration. We did not observe further significant improvements.

As stated previously, we shall not discuss in this paper the SRS (2) with function F given by (8). Rather, we use the IST and incorporate the reconstructed values of constants N_{jkm} and D_{jkm} in the ISRS (7). With F given by (8), this inverse system is readily found to be

$$\dot{x} = \frac{-1}{1+z} \left[-bc + x(a+b) + ya^2 + zc^2 - 2xzc + x^2z \right. \\ \left. + \frac{\sum_{j+k+m=0}^3 N_{jkm} x^j (-y-z)^k (-b-x-ya+zc-xz)^m}{1 + \sum_{j+k+m=1}^3 D_{jkm} x^j (-y-z)^k (-b-x-ya+zc-xz)^m} \right], \quad \dot{y} = x + ay, \quad \dot{z} = b + z(x-c). \quad (10)$$

C. Research of F by using a simplified form

Constants N_{jkm} and D_{jkm} theoretically equal to 0 may be identified on objective grounds, by relying on the following features.

(i) Small values of the corresponding reconstructed constants (see Table I).

(ii) Very big α 's associated with them. When compared with the case of the other constants, these α 's are bigger by more than two orders of magnitude up to more than six orders of magnitude.

(iii) Nonreproducibility of the corresponding evaluations when different time series are processed, in connection with feature (ii).

These two last features indicate that evaluations of the corresponding constants are dominated by numerical noise. Indeed, we check that constants identified as equal to 0 from the above facts are effectively those that are theoretically equal to 0. Dismissing them, Eq. (8) is explicitly rewritten as

TABLE I. Reconstructed numerical values of all constants N_{jkm} and D_{jkm} .

N_{000}	0.795 990 548	D_{100}	-0.227 407 929
N_{100}	-4.180 933 610	D_{010}	-0.000 010 217
N_{010}	0.137 190 166	D_{001}	0.000 017 907
N_{001}	-3.601 912 559	D_{200}	-0.000 020 317
N_{200}	1.909 527 658	D_{020}	-0.000 003 260
N_{020}	0.090 468 385	D_{002}	0.000 029 103
N_{002}	-0.000 188 131	D_{110}	0.000 012 249
N_{110}	-0.759 714 303	D_{101}	0.000 024 532
N_{101}	1.818 842 985	D_{011}	0.000 003 871
N_{011}	-0.227 127 982	D_{300}	0.000 000 898
N_{300}	-0.227 419 943	D_{030}	-0.000 000 146
N_{030}	-0.000 009 593	D_{003}	-0.000 001 651
N_{003}	-0.000 009 775	D_{210}	-0.000 004 700
N_{210}	0.090 485 324	D_{201}	-0.000 012 790
N_{201}	-0.227 483 927	D_{120}	0.000 002 060
N_{120}	0.000 066 128	D_{021}	-0.000 000 029
N_{021}	0.000 039 290	D_{102}	-0.000 011 380
N_{102}	-0.000 045 469	D_{012}	0.000 002 030
N_{012}	-0.000 053 366	D_{111}	0.000 001 332
N_{111}	-0.000 114 238		

$$\begin{aligned} \dot{Z} = & \frac{1}{1 + D_{100}x} (N_{000} + N_{100}x + N_{001}Z + N_{200}x^2 + N_{101}xZ + N_{300}x^3 + N_{201}x^2Z) \\ & + \frac{Y}{1 + D_{100}x} (N_{010} + N_{110}x + N_{020}Y + N_{011}Z + N_{210}x^2) \end{aligned} \tag{11}$$

containing only 13 constants. The problem defined by Eq. (11) could again be solved by the Cramer technique. However, without any significant loss of generality, we shall further decrease the number of constants. For that we may remark from Table I that

$$\begin{aligned} N_{201}/D_{100} &= 1.0003, \\ N_{001}D_{100}/(N_{101} - 1) &= 1.0003, \\ N_{300}/D_{100} &= 1.00005, \\ N_{200} - (N_{100} - D_{100}N_{000})D_{100} &= 0.99991. \end{aligned} \tag{12}$$

Therefore, we may assume on objective grounds that these quantities are equal to 1, although, admittedly, Eq. (12) might have been difficult to find if we did not know what we wanted to do on theoretical grounds. Injecting the four quantities of the left-hand sides of (12), assumed to be equal to 1 in Eq. (11), and reintroducing two constants C and E , we establish after some algebraic calculation that Eq. (11) may be rewritten with 11 constants as

$$\begin{aligned} \dot{Z} = & A + Bx + Cx^2 + ExZ + GZ \\ & + \frac{Y}{1 + Px} (U + Vx + Wx^2 + SY + TZ). \end{aligned} \tag{13}$$

The interesting aspect of this relation with respect to (11) is essentially that it exhibits the same structure as (6). Theoretical expressions and values of constants A, \dots, T are readily derived. To numerically evaluate them, (13) is rewritten under the form

$$\begin{aligned} A + x(AP + B) + YU + ZG + x^2(BP + C) + Y^2S + xYV \\ + YZT + xZ(GP + E) + x^3CP + x^2YW + x^2ZEP \\ + x\dot{Z}(-P) = \dot{Z}, \end{aligned} \tag{14}$$

which now contains 13 constants K_1, \dots, K_{13} linked to constants A, \dots, T .

Again, about ten quadruplets $\{x_i, Y_i, Z_i, \dot{Z}_i\}$ are sampled per pseudoperiod. When 13 quadruplets are recorded, Eq. (14) produces a set of linear equations, which is also solved by the Cramer technique. The set of constants A, \dots, T is afterwards recovered from the set K_1, \dots, K_{13} .

As in Sec. II B, we use a two-step procedure. In the first step, the best series is for $\delta t = 10^{-3}$, $N_s^1 = 20$, leading to an average ϵ per constant (K_1, \dots, K_{13}) equal to 8.10^{-6} and to an average δ per constant equal to 5×10^{-6} , i.e., to a very satisfactory accuracy, much better than that presented in Sec. II B. In the second step, the best series is for $\delta t = 10^{-3}$ and 49 998 quadruplets corresponding to $N_s^2 = 3846$ sets of equations. The average rate of rejection is about 12%. The average ϵ per constant is now 6.5×10^{-6} , representing a significant improvement with respect to the first step but not so impressive as that presented in Sec. II B. The average δ per constant is found to be 3×10^{-7} . Corresponding values for constants A, \dots, T are given in Table II. When one of these constants may be evaluated from two different expressions in terms of K_1, \dots, K_{13} , we retain the evaluation requiring the smallest number of algebraic operations.

As in Sec. II B, we use the IST and incorporate the reconstructed values of constants A, \dots, T in the ISRS (7). With F given by (13), the inverse system is readily found to be

$$\begin{aligned} \dot{x} = \frac{-1}{1+z} \left[(A - Gb - bc) + x(B + a + b - Eb - G) + ya(a - G) + zc(G + c) + x^2(C - E) - xyaE \right. \\ \left. + xz(Ec - G - 2c) + x^2z(1 - E) + \frac{y+z}{1+Px} [(bT - U) + x(T - V) + y(S + aT) + z(S - cT) \right. \\ \left. - x^2W + xzT] \right], \quad \dot{y} = x + ay, \quad \dot{z} = b + z(x - c). \end{aligned} \tag{15}$$

III. VALIDATION OF RESULTS AND DISCUSSIONS

A. Qualitative validation

Qualitative validation relies on the visual comparison between phase portraits. Figure 1 shows a trajectory of

the original Rössler system (1) containing about 10^4 points with about 10^2 points per pseudoperiod. Similarly, Fig. 2 shows a trajectory of the ISRS (10) with the same number of points, the same sampling time, and the same initial conditions as for Fig. 1. Numerical values of reconstructed constants are taken from Table I. We

TABLE II. Reconstructed numerical values of constants A, \dots, T .

A	0.795 996 958
B	-3.999 987 759
C	1.000 004 939
E	1.000 005 590
G	-3.601 987 328
P	-0.227 376 463
U	0.137 243 848
V	-0.759 981 069
W	0.090 496 341
S	0.090 494 834
T	-0.227 374 487

clearly observe that much of the structure of the system has been correctly reconstructed. However, constants being not accurately enough evaluated, the fractal character of the original attractor has been essentially destroyed. Finally, Fig. 3 shows a trajectory of the ISRS (15) with again the same number of points, the same sampling time and the same initial conditions. Numerical values of reconstructed constants are taken from Table II. This figure compares very favorably with the original attractor of Fig. 1. This fact alone would be sufficient to evidence the validity of our methods and algorithms. A more complete discussion, however, requires one to address the issue of structural stability.

B. Structural stability and quality of results

By definition, structural stability concerns the stability of phase portraits under vector field perturbations (see, for instance, Ref. 1, in which the issue is extensively discussed). We may conveniently decompose these perturbations in two cases, namely, (i) perturbations of the mathematical structure itself, i.e., modifications of the mathematical functions appearing in the vector field and of the way in which these functions are combined; and (ii) modifications of the numerical values of constants in-

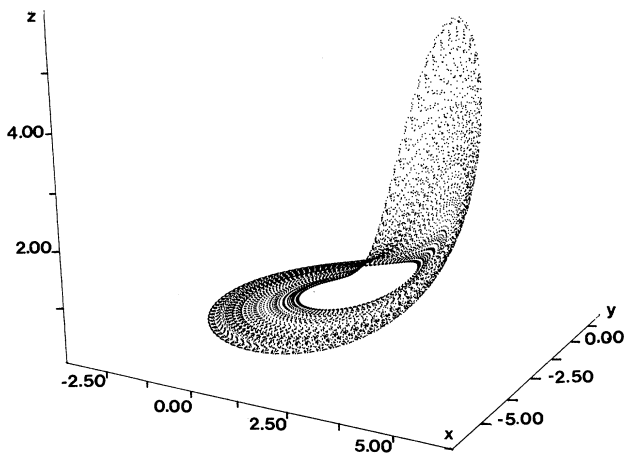


FIG. 1. A trajectory of the original Rössler system (1). Sampling time between two points equal to about 6×10^{-2} .

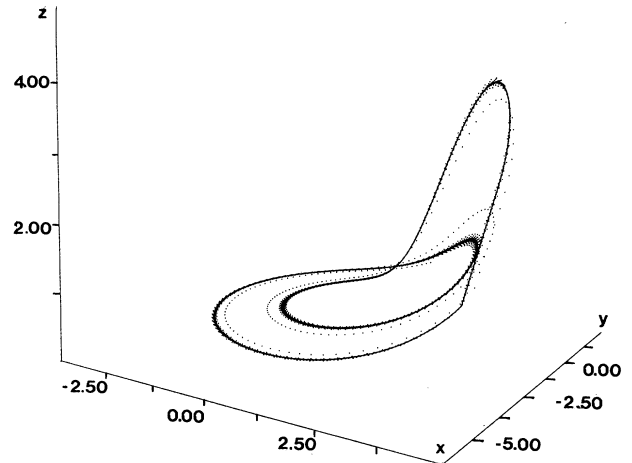


FIG. 2. A trajectory of the inverse standard reconstructed system (10). Sampling time between two points equal to about 6×10^{-2} .

involved in the functions and in their combination. In the framework of bifurcation theory, these constants may be considered as control parameters of the system. Therefore, the purpose of our reconstruction problem is twofold: (i) to correctly identify the mathematical structure, and (ii) to accurately evaluate the control parameters.

For arbitrary systems, we expect, as mentioned above, that the identification of the mathematical structure should require the projection of the standard function F on a complete set of orthogonal functions. The projection process would associate one control parameter with each function.

In the present case, Eq. (8) provides a very decent choice. It is theoretically justified because the Rössler system exhibits this form at order 3. But, knowing only

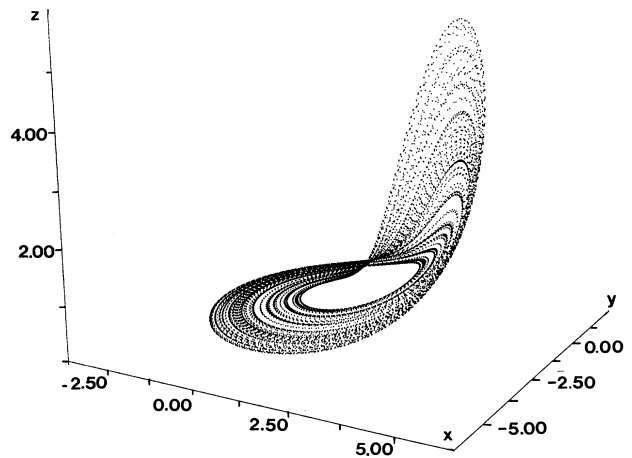


FIG. 3. A trajectory of the inverse standard reconstructed system (15). Sampling time between two points equal to about 6×10^{-2} .

the time series $\{x_i\}$, the validity of the choice is objectively evidenced by the reproducibility of the evaluations of some constants N_{jkm} and D_{jkm} , those which are not theoretically equal to 0, when different time series are analyzed. When noise-dominated constants are preserved, Eq. (8) does not possess exactly the correct mathematical structure, due to the existence of extra parasitic terms, but the associated constants are very small. It would be erroneous to give to these noise-dominated constants the status of control parameters. Dismissing them on objective grounds, Eq. (8) becomes Eq. (11), which now exhibits the correct structure insofar as the number of retained constants is sufficient to describe F and that all constants provide us with relevant information, i.e., there is no noise-dominated constant. However, all constants are not necessary. Using Eqs. (12), the mathematical structure is refined to obtain Eq. (13), which is now structurally perfectly correct, as evidenced by comparison with Eq. (6). The first purpose of the reconstruction, i.e., identification of the mathematical structure, is therefore perfectly fulfilled with Eq. (13) and fairly fulfilled in Eqs. (8) and (11).

In the case of Fig. 2, perturbations of the Rössler vector field concern the two aspects we mentioned: all constants N_{jkm} and D_{jkm} being preserved, small parasitic terms remain, and the other constants are evaluated with an average ϵ per constant which is 0.000 25. Although such an accuracy might be found to be satisfactory in itself, consequences on the phase portrait and on the quality of the reconstructed attractor depend very much on the amount of structural stability. Near a bifurcation locus, even very small errors on constant evaluations may have dramatic effects on phase portraits. In the present case, although constants have been recovered with a fair accuracy, there is at least one bifurcation between Figs. 1 and 2. This bifurcation destroyed the fractal character of the attractor or, at least, modified it deeply. This discussion, however, emphasizes the fact that our methods might be useful for bifurcation predictions of systems when the only available knowledge is a numerical scalar time series. In a general way, whether attractors may be correctly reconstructed will depend, for a given accuracy of constant evaluations, on the structural stability of the system with respect to the addition and omission of terms, and on the proximity of bifurcation loci.

In the case of Fig. 3, the mathematical structure of the vector field is perfectly reconstructed and, furthermore, the average ϵ per constant is very good (6.5×10^{-6}). Both purposes of reconstruction are therefore fulfilled. Metric and dynamical properties of the attractor system could be evaluated in R^3 by using the reconstructed system (see Sec. III C).

Conversely, results could be worse than the ones illustrated by Figs. 2 and 3. For instance, we also used a less efficient finite-difference scheme than the one given by Eq. (3), namely, of the type

$$\dot{x}_i = Y_i = (x_i - x_{i-1})/\delta T, \quad (16)$$

and series $\{x_i, Y_i, \dot{Z}_i, Z_i\}$ were analyzed without using any discrimination scheme.

Then, in the case of Eq. (8), we obtained an average

$\epsilon = 0.02$ per constant not theoretically equal to 0 (with an average δ of 0.015), and an average Δ for the other constants equal to 0.0012. In the case of Eq. (13), the averages ϵ and δ per constant were 0.0064 and 0.0013, respectively. Although these results are not too poor and even identify the mathematical structure as in the previous cases, the corresponding ISRS did not produce correct phase portraits. For instance, Fig. 4 shows a trajectory of the ISRS (15), with initial conditions taken on the Rössler attractor and values of constants obtained by using the scheme (16). This trajectory diverges to infinity. It is likely that the basin of attraction of the attractor has been destroyed or at least deeply modified. For the ISRS (10), divergence to infinity was not obtained when the system motion was tracked on the same observation time, but the trend to divergence was clearly revealed.

One of the most interesting issues and actually our final motivation is the application of vector field reconstructions to experimental systems. In such cases, data are noise polluted. Therefore, even after efficient noise smoothing and removal, we should not expect to identify vector field mathematical structures nor evaluate involved constants with the same accuracy as that found in mathematical models. However, the consequences of such a loss of accuracy might be compensated for by a more robust structural stability of experimental systems, which must resist external noise to be observable.

C. Quantitative validations

In this paper, quantitative validations rely on computations of generalized dimensions. Definitions and the algorithms used are briefly recalled for completeness.

We consider an attractor A and a partition of A into boxes of size r . The boxes are numbered from 1 to $M(r)$. Let p_i be the probability measure of box i . Generalized dimensions D_q are defined by (see Refs. 8–10, 39–41, and references therein)

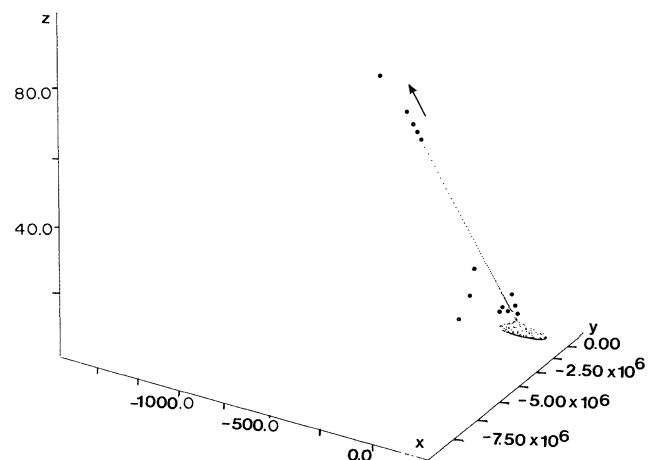


FIG. 4. An example of a trajectory of a poor quality inverse standard reconstructed system showing divergence to infinity.

$$D_q = \frac{1}{q-1} \lim_{r \rightarrow 0} \left[\frac{\log \sum_{i=1}^{M(r)} p_i^q}{\log r} \right]. \quad (17)$$

We define a local correlation $C_i(r)$ at point $X(i)$ by the relation

$$C_i(r) = \frac{1}{N-1} nb \{j \neq i, |X(i) - X(j)| \leq r\}. \quad (18)$$

In this relation, $X(i)$ is a vector, which will be (x_i, y_i, z_i) for the original Rössler system or for the ISRS. N is the size of the temporal sequence, i.e., the number of vectors in it, and j ranges from 1 to N . $|\cdot|$ is a norm to compute the distance between vectors $X(i)$ and $X(j)$. We use the ∞ norm, i.e., the maximum among the absolute values of the component differences.

We consider m central vectors chosen at random with respect to the natural measure and define order- q correlations $C_q(r)$ by spatially averaging local correlation moments, according to

$$C_q(r) = \frac{1}{m} \sum_{i=1}^m C_i^q(r), \quad q \neq 1 \quad (19)$$

and, for the special case $q=1$,

$$C_1(r) = \left[\prod_{i=1}^m C_i(r) \right]^{1/m}. \quad (20)$$

Assuming that the measure is ergodic on the attractor, we then show that

$$\lim_{r \rightarrow 0} C_q(r) \simeq r^{QD_q}, \quad (21)$$

in which Q is $q-1$ for $q \neq 1$ and 1 for $q=1$.

Ideally, the size N of the temporal sequence and the number m of central vectors must tend towards the infinite to reach the limit $r \rightarrow 0$ in Eq. (21). In practice, computations are carried out with a finite resolution (N, m) and preferably with the condition $m \leq N$. Then the scaling equation (21) is only observed for a finite r -scaling domain.

Therefore, C_q 's are evaluated at discrete values r_i of r , (preferably) separated by equal distances in logarithmic scales. Local values of D_q 's at r_i 's are then evaluated in the r -scaling domain by computing local slopes

$$D_q(r_i) = \frac{1}{Q} \frac{\log[C_q(r_i + \Delta r_i)/C_q(r_i - \Delta r_i)]}{\log[(r_i + \Delta r_i)/(r_i - \Delta r_i)]}. \quad (22)$$

D_q 's are afterward obtained by averaging local slopes in the r -scaling domain. We obtain an insight into the accuracy of the results from the standard mean deviation of the local slope values.

The above algorithm is implemented in computer programs to study the original Rössler system (1) and the ISRS (10) and (15) corresponding to Figs. 1, 2, and 3, respectively. Computations are carried out with a Runge-Kutta time step $\delta t = 10^{-3}$. About 60 vectors are sampled per pseudoperiod T_0 . Local slopes $D_q(r_i)$ are evaluated on 45 r_i locations separated by equal logarithmic inter-

vals on a range (r_{\min}, r_{\max}) .

For system (1) of Fig. 1, D_q computations are carried out for q ranging from (-50) to $(+50)$. It is well known that the choice of the r scaling domain lacks objectivity in this algorithm and that this feature is actually one of its shortcomings. Furthermore, (r_{\min}, r_{\max}) depend on q . Therefore, a new table should ideally be given. We may, however, roughly indicate these domains by stating that they are about $(0.06-0.25)$ for $q \in [-50, -9.75]$ and about $(0.045-0.23)$ for $q \in]-9.75, +50]$, to compare with the extension of the Rössler attractor given by $\Delta x \simeq 8.5$, $\Delta y \simeq 7.7$, and $\Delta z \simeq 6.1$. For the sake of accuracy, computations are performed with a high resolution $(N, m) = (10^6, 2000)$ after having performed preliminary indicative runs at smaller resolutions $(5 \cdot 10^4, 200)$ and $(10^5, 500)$.

D_q computations are similarly carried out for the ISRS of Eq. (15) and Fig. 3, under exactly the same specifications as in the previous case, including the choice of the r -scaling domains. Results are presented in Fig. 5. We observe that D_q decreases when q increases, in agreement with known results from the theory of generalized dimensions. We also remark that displayed D_q 's become smaller than 2 for q larger than about 0. In particular, the correlation dimensions D_2 are 1.88 and 1.91 for the original system and for the ISRS, respectively. These D_2 values are not satisfactory for hyperbolic strange attractors, but our D_2 value for the Rössler attractor agrees perfectly well with results mentioned in Ref. 26 and obtained with the same algorithm. Indeed, underestimations of dimensions are also a classical feature of the algorithm. Some statistical error bars are displayed in the figure. They greatly increase when q becomes large or small. However, these error bars are only a clue to statistical accuracy and should not be given a too serious meaning. See Ref. 28 for similar observations concerning D_q underestimations and error-bar behavior in the case of a strange attractor produced by a model of thermal lens oscillations. We are, however, more interested in comparing systems than in absolute evaluations of dimensions. Such comparisons make sense because the algorithm is run under the same specifications for both the Rössler system and the ISRS. Then, Fig. 5 displays a very satisfactory agreement, evidencing that metric properties are correctly recovered. The relative difference for D_2 is about 1.5%. Even for extreme q 's, it remains small, being 0.9% for $q = +50$ and less than 2% for $q = -50$.

For the ISRS of Eq. (10) and Fig. 2, we should not expect such a good agreement. In this case, computations have been carried out with smaller resolutions and only D_0 (capacity), D_1 (information dimension), and D_2 (correlation dimension) have been evaluated. For $(N, m) = (5 \times 10^4, 200)$ we find that all these dimensions are equal to 1.01 ± 0.02 in an r -scaling domain $(r_{\min}, r_{\max}) = (0.025, 0.53)$.

Therefore, over more than two orders of magnitude of r , the attractor is not fractal. Dimensions equal to 1 are in agreement with Fig. 2, showing that the orbit is essentially periodic. However, we also observe that the attractor might be fractal at smaller scales. We effectively computed that local slopes $D_q(r_i)$ approach 1.8 for r near

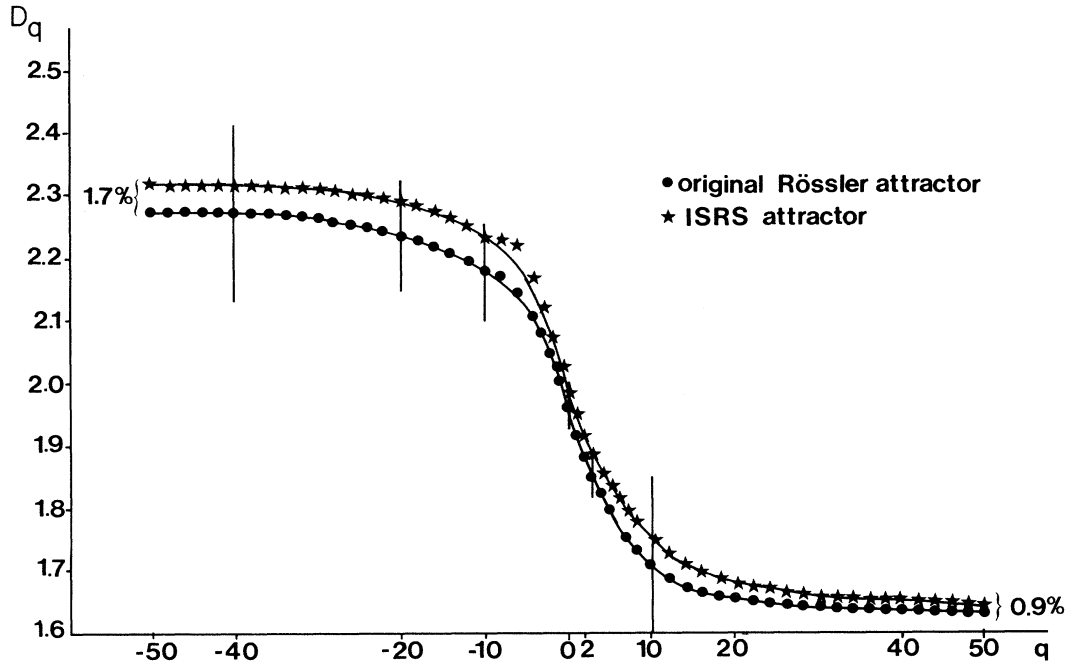


FIG. 5. Satisfactory comparison between generalized dimensions D_q of the original Rössler system and of the ISRS of Eq. (15).

0.001. Accounting for underestimations due to finite resolution, these local slopes might actually be larger than 2. Another clue to the existence of residual chaos at small scales might be the fact that some parts of the orbit leave the main band. The most likely diagnostic concerning this attractor is that it is chaotic with large lacunarity and chaos confined to small scales near a periodic orbit. A more complete investigation of this object is, however, not interesting in the framework of the present paper.

IV. CONCLUSION

We have emphasized that the knowledge of numerical scalar time series permits the reconstruction of the equations of the underlying dynamical system or, at least, of equivalent ones. This result opens the way to many lines of research, some of them having been mentioned in this paper. Although some of our suggestions might be optimistic, an interest in a more complete examination of

them is warranted.

In our opinion, the most interesting prospect might be the possibility of automatic reconstruction of phenomenological models. Although more work should be devoted to the study of mathematical models, particularly with the addition of noise, in order to improve and generalize algorithms, the final motivation is the study of experimental systems. With such a motivation in mind, we now intend to systematically exploit the opportunities offered by the results we presented. More details, including computer program sources, are contained in an internal report available on request.

ACKNOWLEDGMENT

The Laboratoire d'Energétique des Systèmes et Procédés is "associé au Centre National de la Recherche Scientifique, No. 230."

- ¹J. Guckenheimer and P. Holmes, *Nonlinear Oscillations, Dynamical Systems and Bifurcations of Vector Fields*, Vol. 52 of *Applied Mathematical Sciences*, edited by F. John, J-E. Marsden, and L. Sirovich (Springer-Verlag, Berlin, 1983).
- ²J. M. T. Thompson and H. B. Stewart, *Nonlinear Dynamics and Chaos* (Wiley, New York, 1987).
- ³R. L. Devaney, *An Introduction to Chaotic Dynamical Systems* (Addison-Wesley, Reading, MA, 1987).
- ⁴P. Bergé, Y. Pomeau, and C. Vidal, *L'Ordre dan le Chaos* (Hermann, Paris, 1984).

- ⁵J. D. Farmer, E. Ott, and J. A. Yorke, *Physica* **7D**, 153 (1983).
- ⁶A. Wolf, J. B. Swift, H. L. Swinney, and J. A. Vastano, *Physica* **16D**, 285 (1985).
- ⁷P. Grassberger, R. Badii, and A. Politi, *J. Stat. Phys.* **51**, 135 (1988).
- ⁸H. G. E. Hentschel and I. Procaccia, *Physica* **8D**, 435 (1983).
- ⁹P. Grassberger and I. Procaccia, *Physica* **13D**, 34 (1984).
- ¹⁰R. Badii and A. Politi, *J. Stat. Phys.* **4**, 725 (1985).
- ¹¹T. Morita, H. Hata, H. Mori, T. Horita, and K. Tomita, *Prog. Theor. Phys.* **79**, 296 (1988).

- ¹²W. Van de Water and P. Schram, *Phys. Rev. A* **37**, 3118 (1988).
- ¹³J. G. Caputo and P. Atten, *Phys. Rev. A* **35**, 1311 (1987).
- ¹⁴C. Grebogi, E. Ott, and J. A. Yorke, *Phys. Rev. A* **37**, 1711 (1988).
- ¹⁵D. Auerbach, Ben O'Shaughnessy, and I. Procaccia, *Phys. Rev. A* **37**, 2234 (1988).
- ¹⁶G. Broggi, *J. Opt. Soc. Am. B* **5**, 1020 (1988).
- ¹⁷M. Ravani, B. Derighetti, G. Broggi, and E. Brun, *J. Opt. Soc. Am. B* **5**, 1029 (1988).
- ¹⁸Y. Termonia, *Phys. Rev. A* **28**, 2591 (1983).
- ¹⁹Y. Termonia, *Phys. Rev. A* **29**, 1612 (1984).
- ²⁰R. Mañé, in *Dynamical Systems and Turbulence, Warwick, 1980*, Vol. 898 of *Lecture Notes in Mathematics*, edited by D. A. Rand and L. S. Young (Springer-Verlag, Berlin, 1981), pp. 230–242.
- ²¹F. Takens, in *Dynamical Systems and Turbulence, Warwick, 1980* (Ref. 20), pp. 366–381.
- ²²F. Takens, in *Nonlinear Dynamics and Turbulence*, edited by G. I. Barenblatt, G. Iooss, and D. D. Joseph (Pitman, New York, 1983), pp. 314–332.
- ²³J. P. Eckmann, *Rev. Mod. Phys.* **57**, 617 (1985).
- ²⁴D. S. Broomhead and G. P. King, *Physica* **20D**, 217 (1986).
- ²⁵A. M. Albano, J. Muench, and C. Schwartz, *Phys. Rev. A* **38**, 3017 (1988).
- ²⁶P. S. Landa and M. G. Rozenblyum, *Zh. Tekhn. Fiz. [Sov. Phys.—Tech. Phys.]* **34**, (1),6 (1989).
- ²⁷A. M. Fraser, *Physica D* **34**, 391 (1989).
- ²⁸G. Gouesbet, *Phys. Rev. A* **42**, 5928 (1990).
- ²⁹M. Casdagli, *Physica D* **35**, 335 (1989).
- ³⁰G. Gouesbet and E. Lefort, *Phys. Rev. A* **37**, 4903 (1988).
- ³¹G. Gouesbet, M. E. Weill, and E. Lefort, *AIAA J.* **24**, 1324 (1986).
- ³²G. Gouesbet, *J. Jpn. Soc. Mech. Eng.* **32**, Ser. II, 301, (1989).
- ³³G. Gouesbet, *Entropie*, **153/154**, 47 (1990).
- ³⁴J. D. Farmer and J. J. Sidorowich, *Phys. Rev. Lett.* **59**, 845 (1987).
- ³⁵N. H. Packard, J. P. Crutchfield, J. D. Farmer, and R. S. Shaw, *Phys. Rev. Lett.* **45**, 712 (1980).
- ³⁶J. Cremers and A. Hübler, *Z. Naturforsch.* **42A**, 797 (1987).
- ³⁷H. Froehling, J. P. Crutchfield, D. Farmer, N. H. Packard, and R. Shaw, *Physica* **3D**, 605 (1981).
- ³⁸A. Cenys and K. Pyragas, *Phys. Lett. A* **129**, 227 (1988).
- ³⁹P. Grassberger, *Phys. Lett.* **97A**, 227 (1983).
- ⁴⁰A. Cohen and I. Procaccia, *Phys. Rev. A* **31**, 1872 (1985).
- ⁴¹C. Grebogi, E. Ott, S. Pelikan, and J. A. Yorke, *Physica* **13D**, 261 (1984).